Investigation of Canadian seismic code requirements for reinforced concrete frames

P.Paultre
Les Consultants Dessau, Inc., Laval, Quebec, Canada

D.Mitchell
McGill University, Montreal, Quebec, Canada

Abstract: Three full-scale reinforced concrete beam-column-slab subassemblages were tested in order to investigate the seismic design and detailing requirements of the Canadian Concrete Code. Predicted and measured responses are compared and the role of the slabs, joints and the spandrel beams are investigated. Some suggestions for design are given. The results of non-linear analyses of six story frame structures designed with three different levels of ductility are presented.

1 INTRODUCTION

The 1984 Canadian Concrete Code (Canadian Standards Association 1984) introduced new seismic design and detailing requirements for reinforced concrete structures. The design provisions for ductile moment resisting frame members (K = 0.7) were revised and new provisions were presented for members with "nominal ductility" (K = 1.3). The research reported in this paper is part of an overall study of the seismic behaviour of reinforced concrete structures in Canada. As part of this study a number of reinforced concrete frame structures with varying degrees of ductility (K = 2.0, K = 1.3 and K = 0.7) were designed for Montreal and Vancouver (See Fig. 1). Full scale test specimens representing the second floor exterior beam-column-slab sub-assemblage of the Montreal frame structures were built and tested. The purpose of these tests was to investigate the behaviour of members with different levels of ductility and to develop general behavioural models capable of estimating the full response of these members. These behavioural models enabled non-linear dynamic analyses of the series of frame structures to be performed.

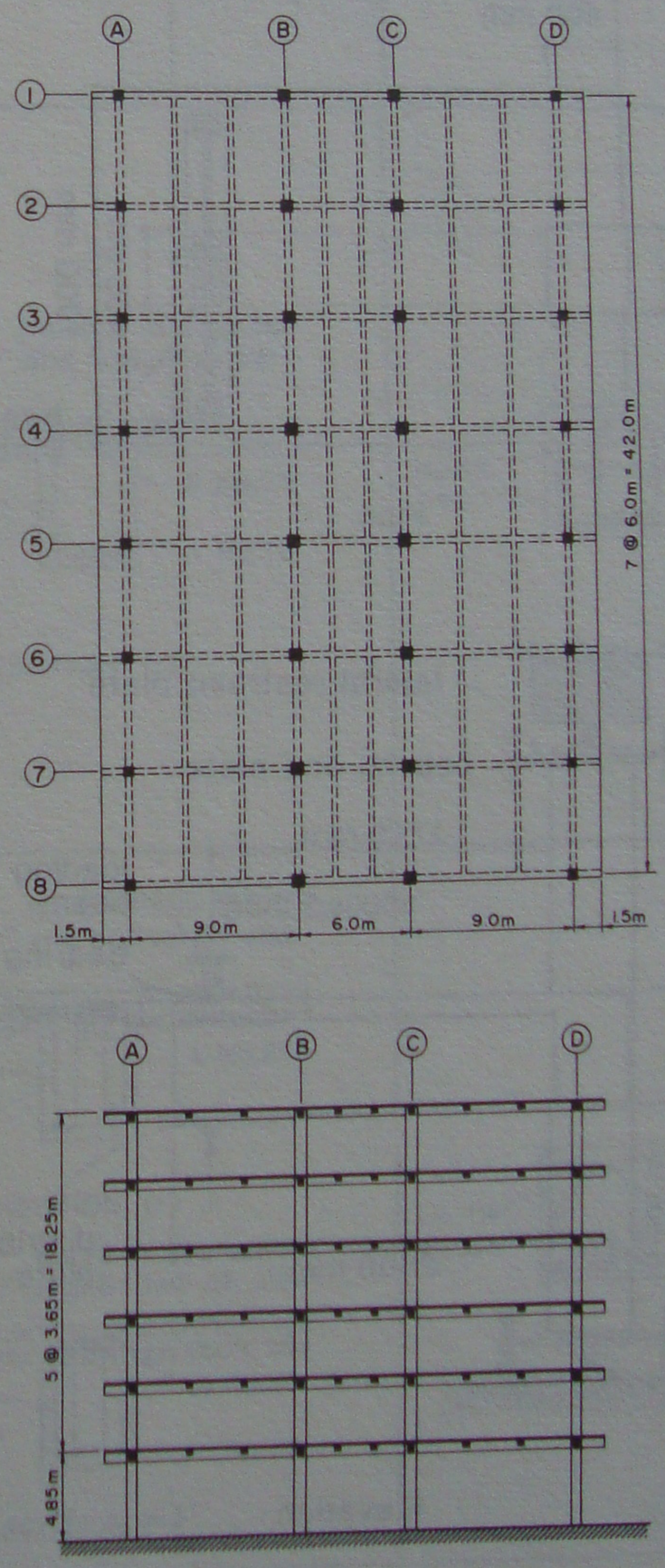

Fig. 1. Six storey frame structure.

2 TEST SPECIMENS

Three full scale test specimens designed and detailed for K = 2.0 (Specimen K2.0),

K = 1.3 (Specimen K1.3) and K = 0.7 (Specimen K0.7) were tested. The overall dimensions and test set-up for all three specimens are shown in Fig. 2. The test set-up permits reversed cyclic loading to be applied to the sub-assemblage while a constant compressive axial load of 1076 kN (90% of the dead load) is applied to the 450 X 450 mm column. As can be seen the slab and spandrel beams were also included in the specimens. Figure 3 summarizes the reinforcement details for the three specimens. Specimen K2.0 contained reinforcing bars meeting the requirements of CSA G30.12 (Canadian Standards Association 1977a) while specimens K1.3 and K0.7 contained weldable low alloy reinforcing bars meeting the requirements of CSA G30.16 (Canadian Standards Association 1977b). The properties of the Grade 400 reinforcing bars are presented in Table 1.

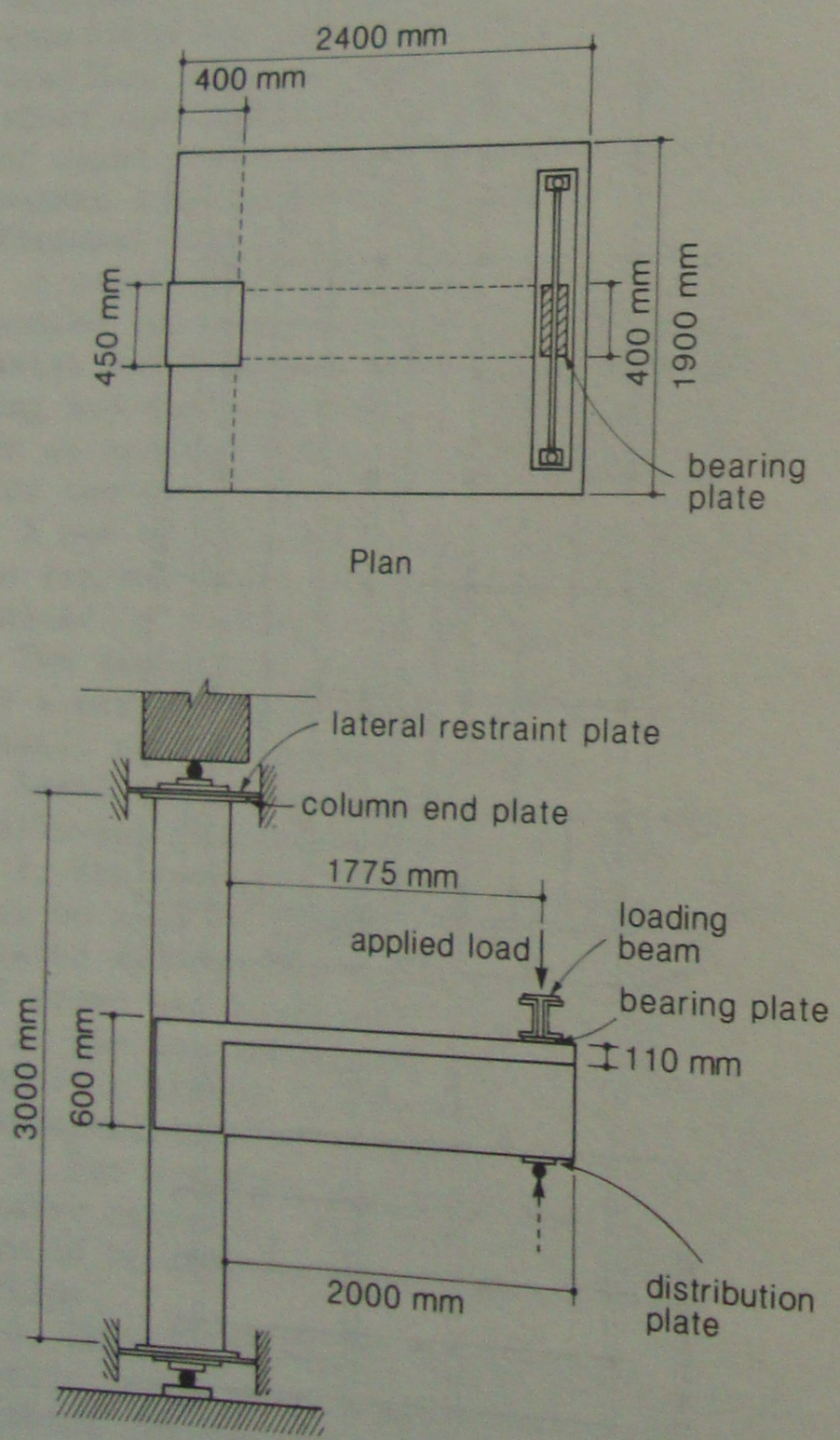

Fig. 2. Test set-up.

Table 1. Reinforcing bar properties.

Size	Area mm^2	Yield Stress MPa
# 3*	71	406
No.10*	100	492
No.10	100	480
No.15*	200	400
No.15	200	472
No.20	300	478

* Specimen K2.0 only

The average concrete strengths for specimens K2.0, K1.3, and K0.7 were 39.8 MPa, 39.5 MPa and 40.4 MPa respectively. The instrumentation consisted of the following:

1. Load cells.
2. LVDT's for measuring beam tip deflections.
3. Mechanical strain targets on the slab reinforcing bars, on the top and bottom of the beam along its length to determine curvatures and also in the form of rosettes on the side face of the beam along its length to determine shear strains.
4. Dial gauges at the column-slab connection to determine bond slip and joint shear distortion.

Loading was applied to predetermined load levels up to general yielding. The peak loading in subsequent cycles was controlled by deflection with maximum deflection levels taken as multiples of the deflection measured at general yielding.

3 TEST RESULTS

Figure 4 shows the load vs. beam tip deflection responses for the three specimens. As can be seen in Fig. 4a specimen K2.0 exhibited a significant decrease in load capacity as well as a large stiffness reduction and severe pinching of the response curves after a displacement ductility of about 3. This was due to both severe shear distress and buckling of the bottom longitudinal bars between the widely spaced stirrups (see Fig. 5a).

Specimen K1.3 exhibited a slight loss of load carrying capacity after a displacement ductility of about 3 (see Fig. 4b) due to spalling of the cover

concrete at the bottom of the beam. The testing had to be stopped after achieving a displacement ductility of 5 due to failure of the joint region (see Fig. 5b). Specimen K0.7 exhibited stable hysteric response throughout the duration of the testing and maintained its load carrying capacity in both loading directions (see Fig. 4c). Testing had to be stopped due to lack of travel of the loading apparatus at a displacement ductility of 8. Figure 5c shows specimen K0.7 at this stage.

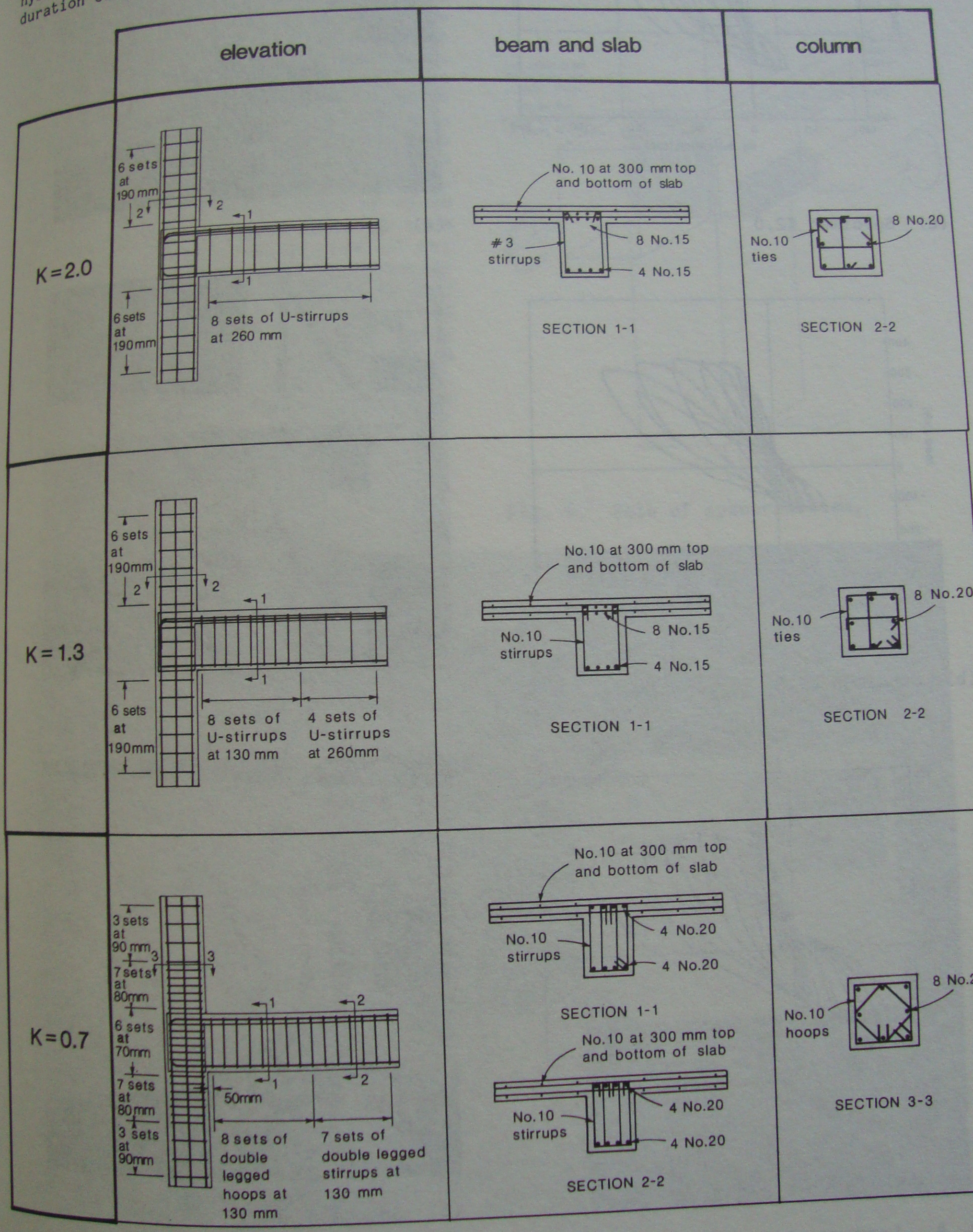

Fig. 3. Specimen reinforcement details.

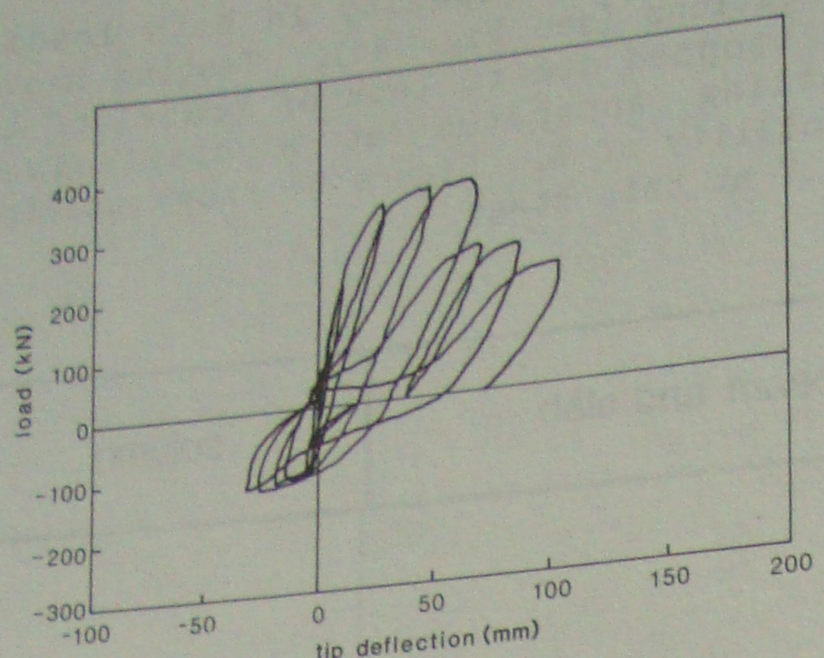

(a) Specimen K2.0

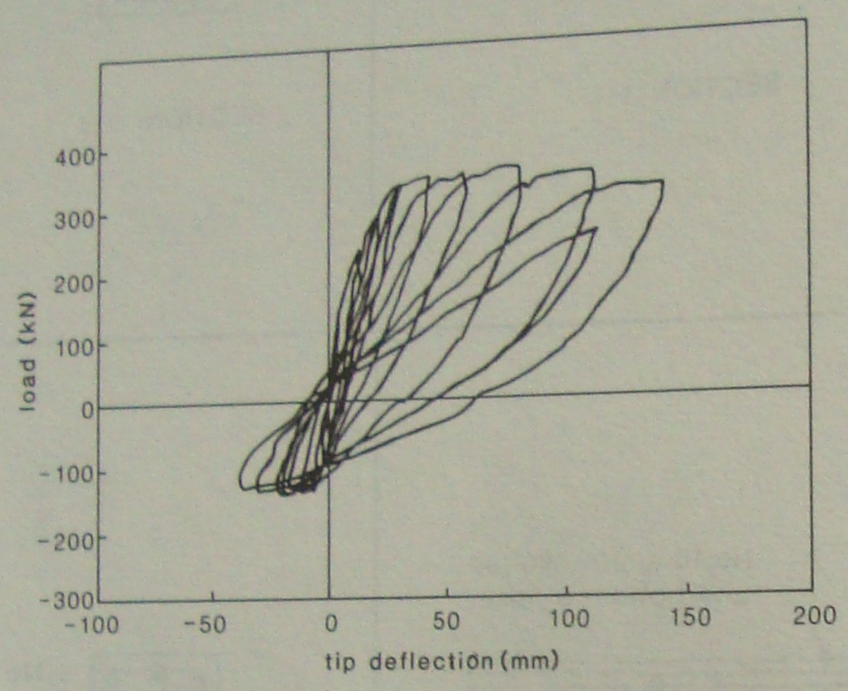

(b) Specimen K1.3

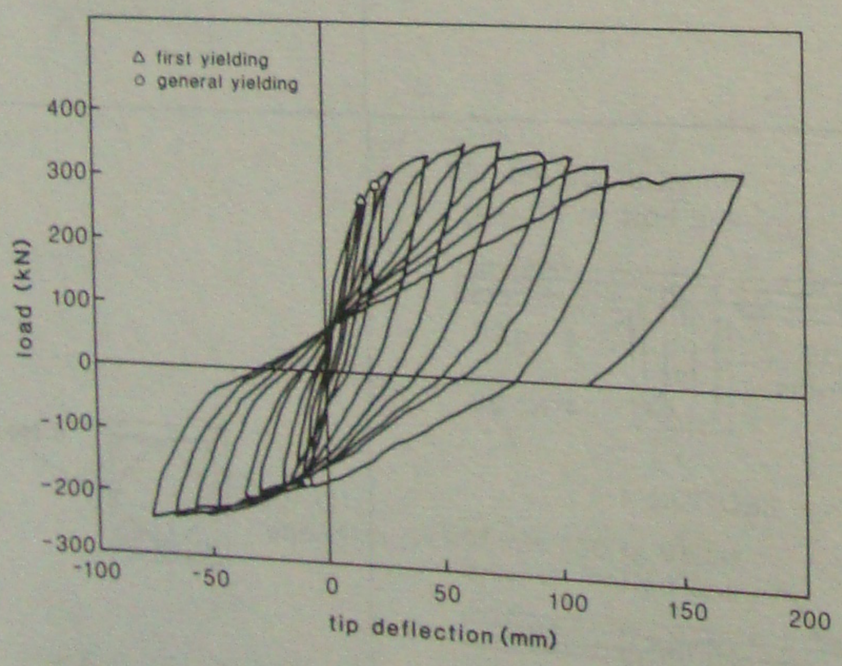

(c) Specimen K0.7

Fig. 4. Load vs. tip deflection responses.

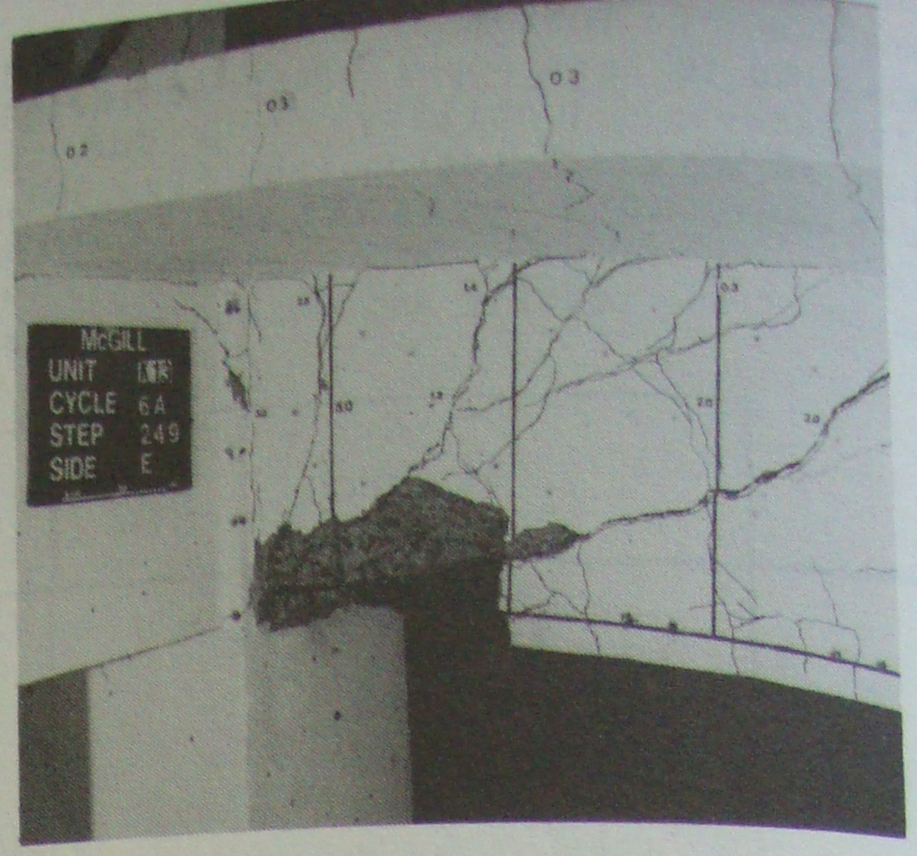

(a) Specimen K2.0

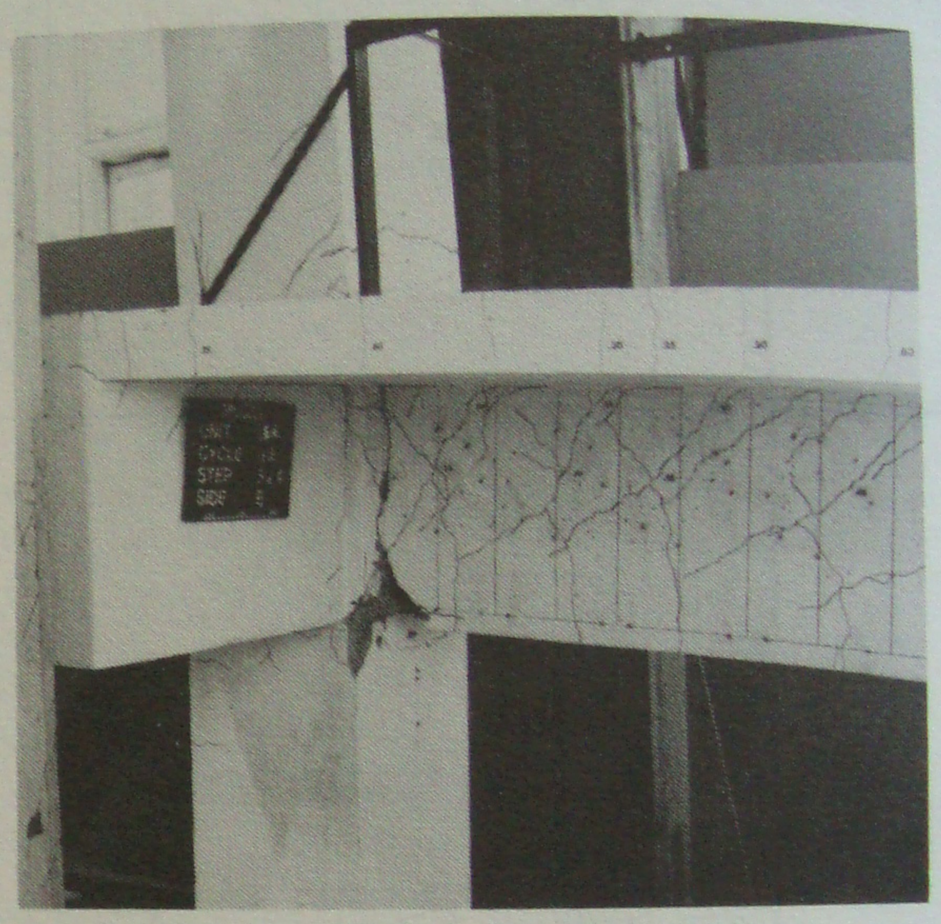

(b) Specimen K1.3

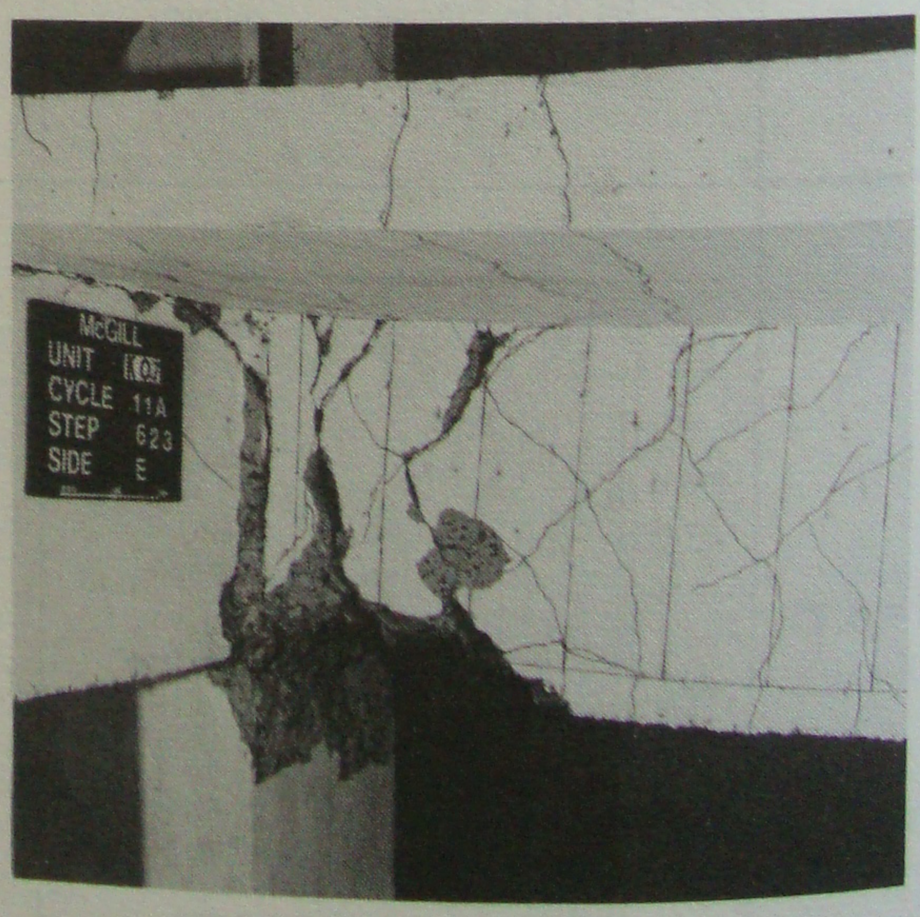

(c) Specimen K0.7

Fig. 5. Specimens near failure.

4 ROLE OF SPANDREL BEAM

Figure 6 illustrates the flow of the forces from the slab and the main beam into the joint region. The tensions in the slab bars from bending of the main beam create torsion in the spandrel beams which in turn transmit both direct shear and torsional shear flow to the side faces of the joint. The total tension in the slab bars will therefore be limited by the torsional capacity of the spandrel beam. For example the torsional capacity of the spandrel beam in specimen K1.3 is about 99,000 kN·m and since the slab bars are located 245 mm from the centre of the beam the maximum tensile force that can be transmitted is 99,000/0.245 = 404 kN. Since each bar has a yield force of 48 kN this total force corresponds to 8.4 bars at the yield level on each side of the column. From the strain measurements all 6 bars on each side of the column yielded at failure and some bars had reached strain hardening. Due to the large torsional cracks observed in the spandrel beams of all three specimens it is evident that they all yielded in torsion (e.g. see Fig. 7).

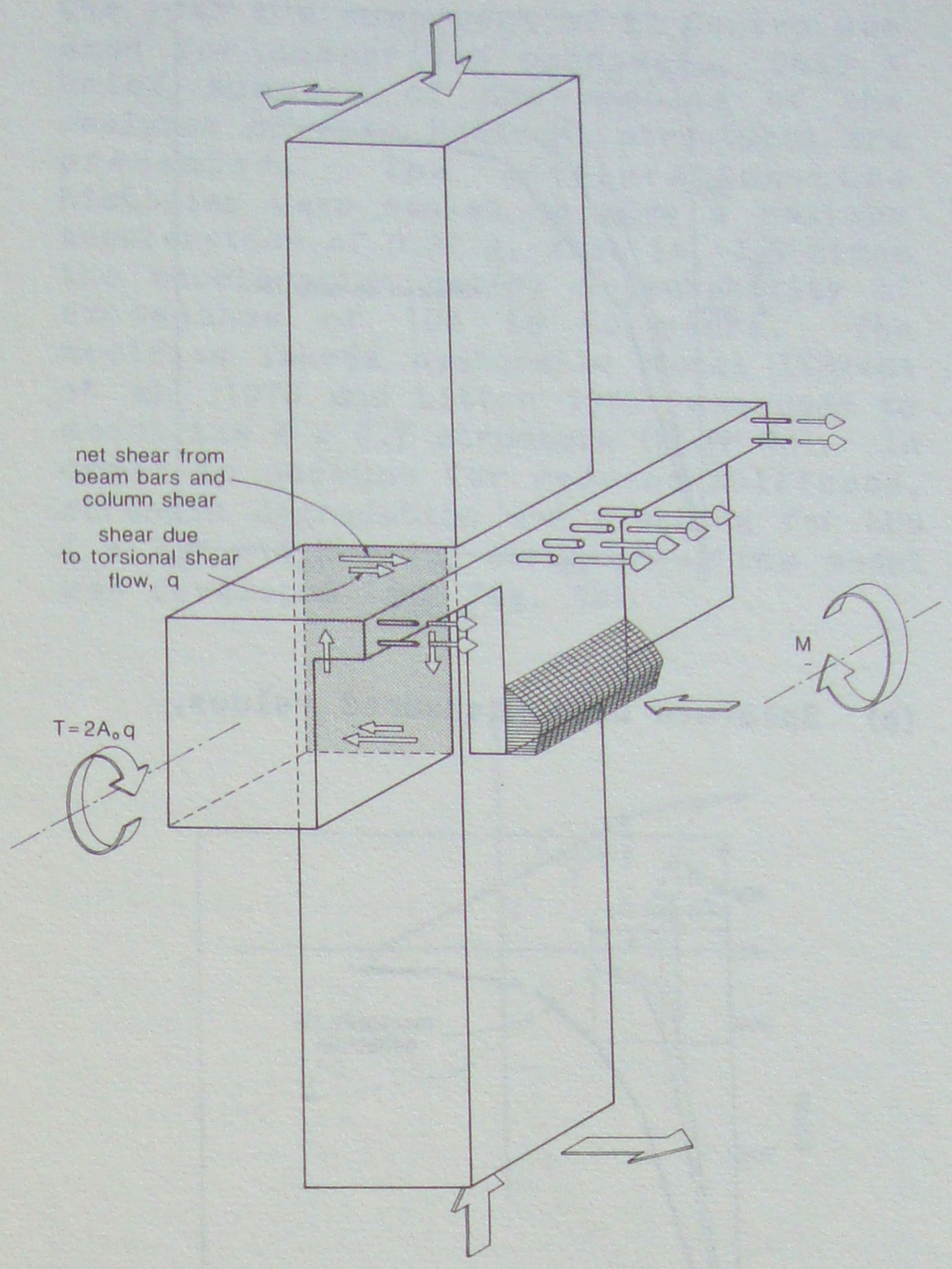

Fig. 6. Role of spandrel beam.

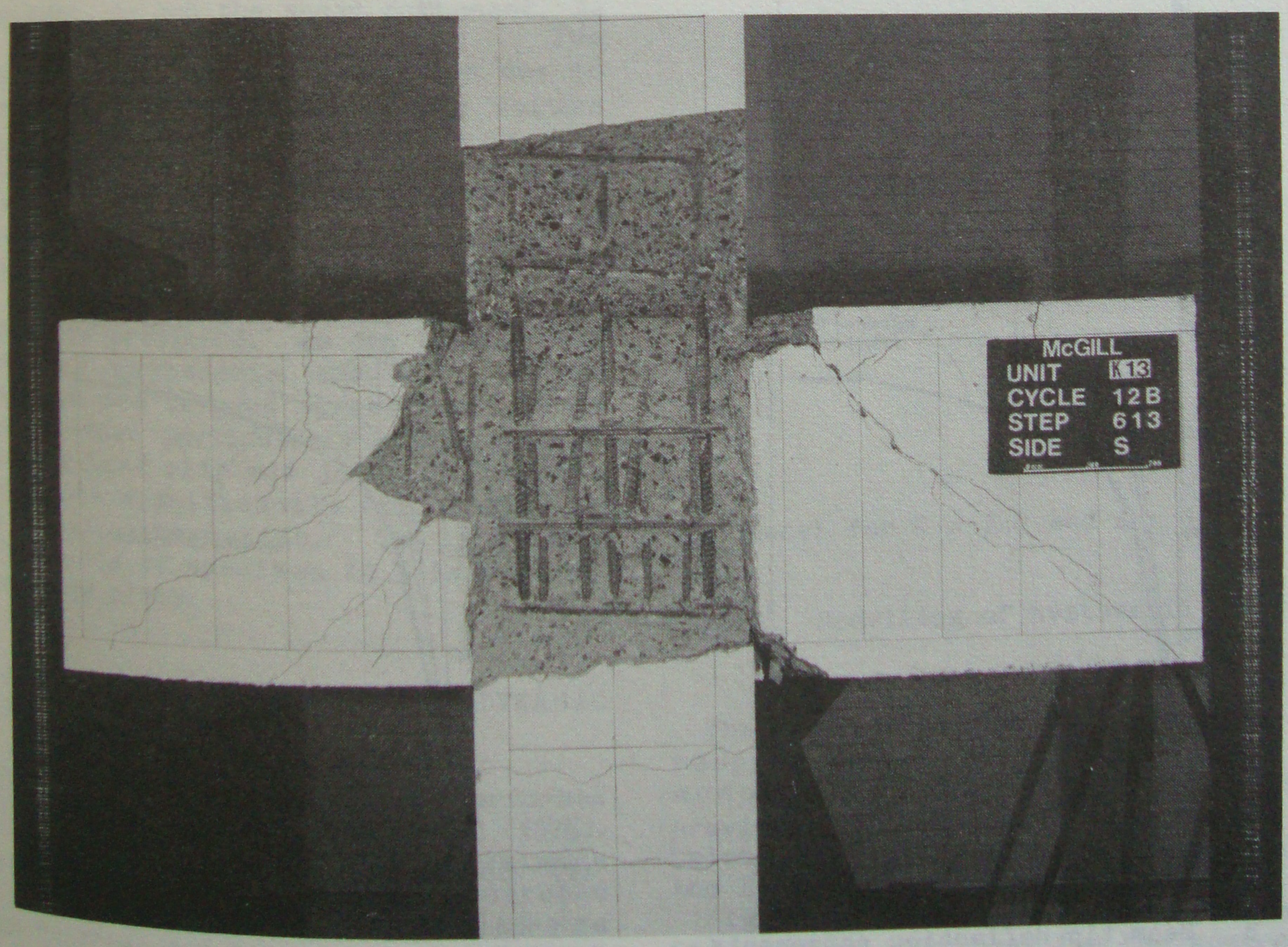

Fig. 7. Exterior face of specimen K1.3.

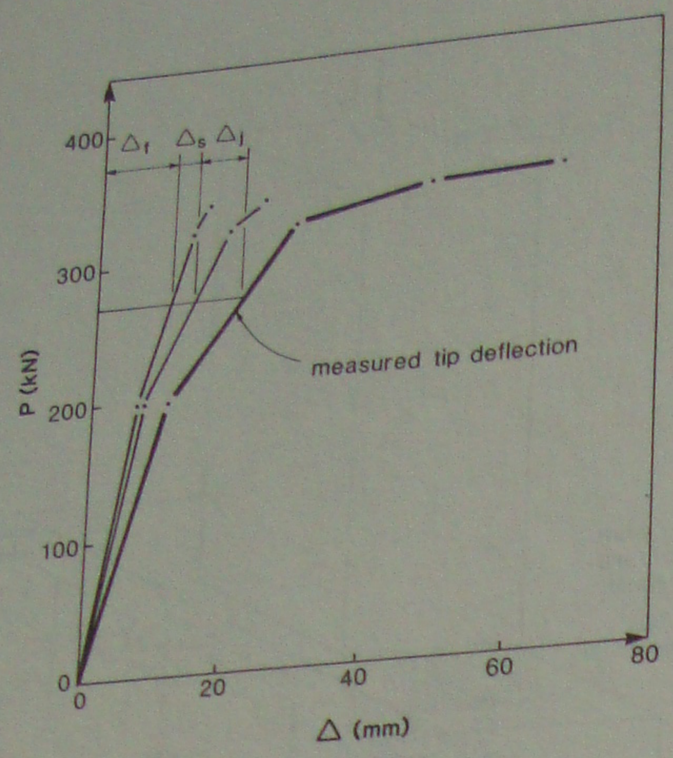

(a) Specimen K2.0, measured values.

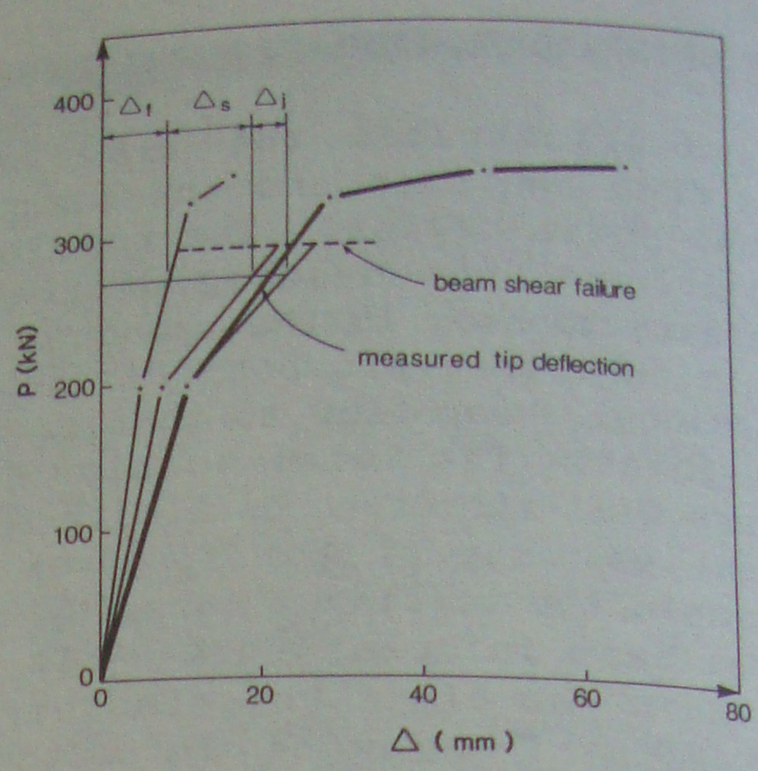

(b) Specimen K2.0, predicted values.

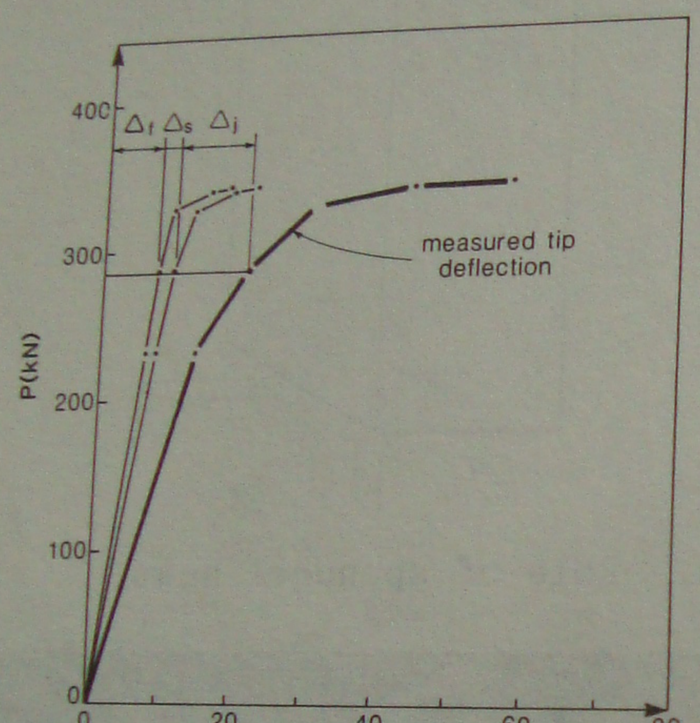

(c) Specimen K1.3, measured values.

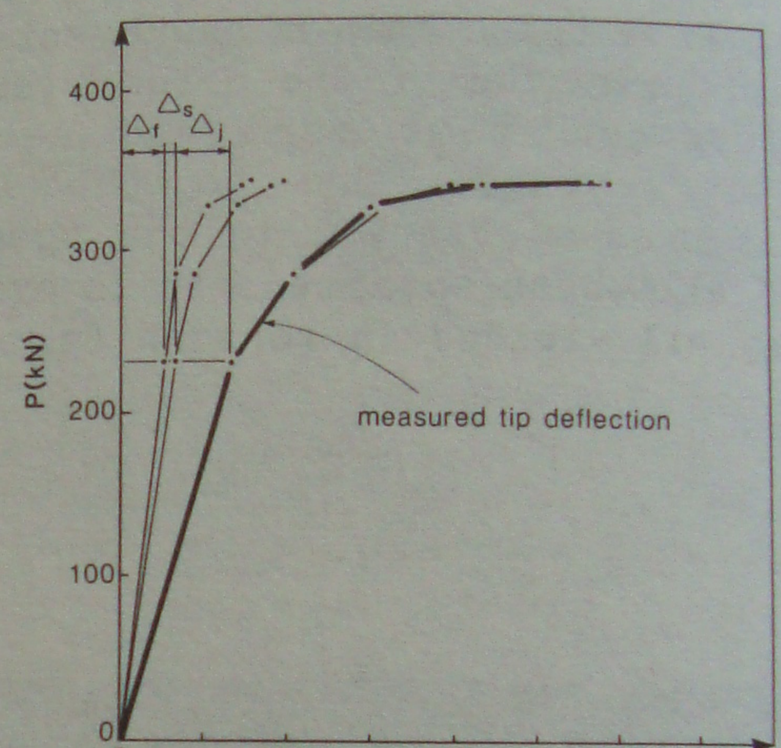

(d) Specimen K1.3, predicted values.

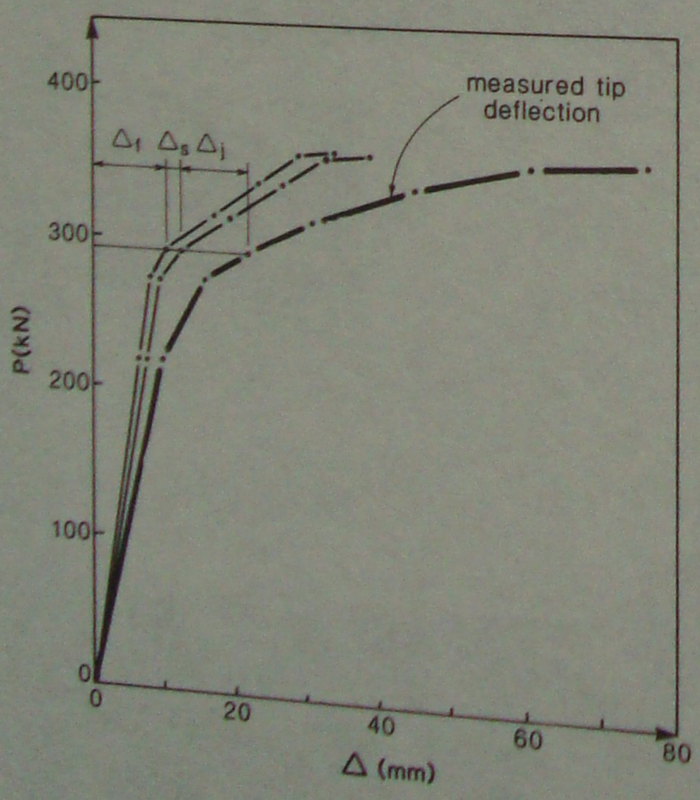

(e) Specimen K0.7, measured values.

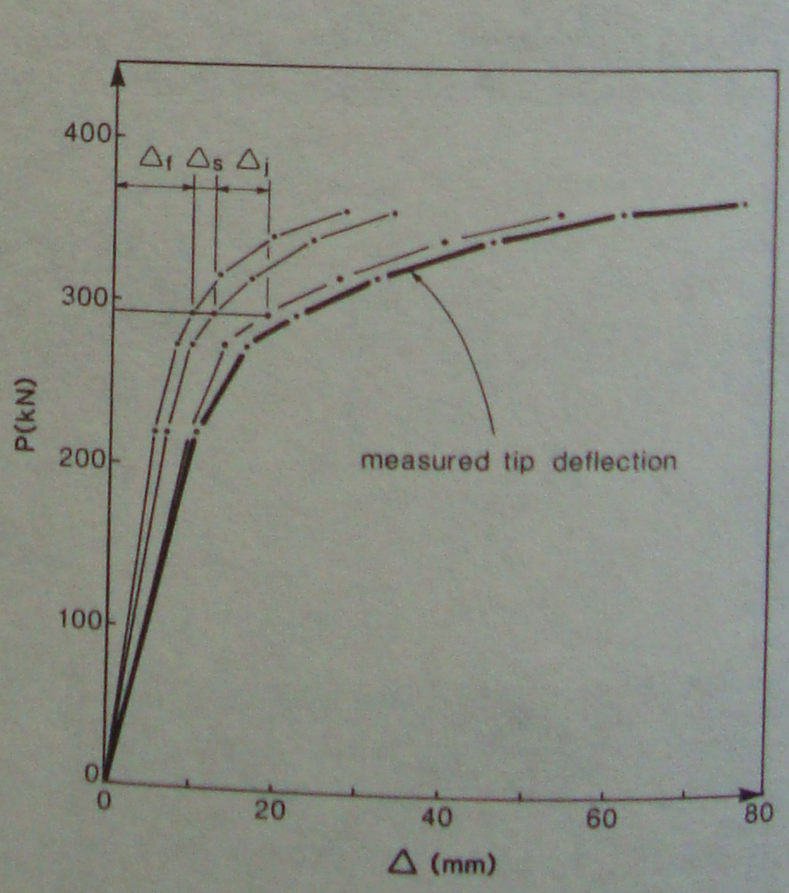

(f) Specimen K0.7, predicted values.

Fig. 8. Beam tip deflection components.

5 PREDICTING SUBASSEMBLAGE RESPONSES

Detailed behavioural models, (Paultre 1987) were developed to predict the responses of the members of the subassemblages as described below :

1. A general purpose computer program was developed to predict the axial load-flexural response of sections accounting for (a) the complete stress-strain relationship of the steel, (b) the influence of confinement and tension stiffening on the stress-strain relationship of the concrete, (c) progressive spalling of the concrete cover and (d) the non-linear strain distribution in flanges.

2. A computer program was developed to account for the combined effects of flexure, axial load and shear in order to predict the sectional responses, that is, shear deformations (Collins and Mitchell 1985) and curvatures. This model was used to predict the shear distortion in the beams and the joints.

3. A simple bi-linear bond slip model was used to estimate this contribution.

The behavioural models were used to predict the sectional response at different locations along lengths of the beam. The resulting distributions of curvature and shear strains were then integrated to determine the flexural component, Δ_f and the shear component, Δ_s of the beam tip deflection. The contribution to the tip deflection due to a concentrated rotation at the column face, Δ_j, were determined from the predicted bond slips and joint shear strains.

Figure 8 compares the measured contributions of the components (i.e. Δ_f, Δ_s and Δ_j) to the beam tip deflection with those predicted. As can be seen the predicted components and the overall responses are in good agreement. It is apparent that particularly after general yielding bond slip and joint distortion contribute significantly (about 50%) to the total deformation. The improved performance of specimen K0.7 is evident from these plots.

6 PREDICTIONS OF NON-LINEAR DYNAMIC RESPONSES OF STRUCTURES

Non-linear dynamic analyses were performed using DRAIN-2D (Kanaan and Powell 1975). Three acceleration-time histories were chosen from 12 artificially generated histories matching the response spectra from Montreal and Vancouver. In addition the 1940 E-W component of El Centro was used for comparison purposes. Only a brief summary of the results of the analyses of some Montreal structures are presented. The acceleration-time histories were scaled to give a maximum acceleration of 0.27 g, that is, 1.5 times the acceleration having a probability of exceedance of 10% in 50 years. The modified Takeda hysteretic model (Takeda et al. 1970 and Litton 1975) was used to model the K = 0.7 structure (Fig. 9a). In order to account for reduced stiffness, strength degradation and pinching for the K = 2.0 and K = 1.3 structure a new model was developed (see Fig. 9b).

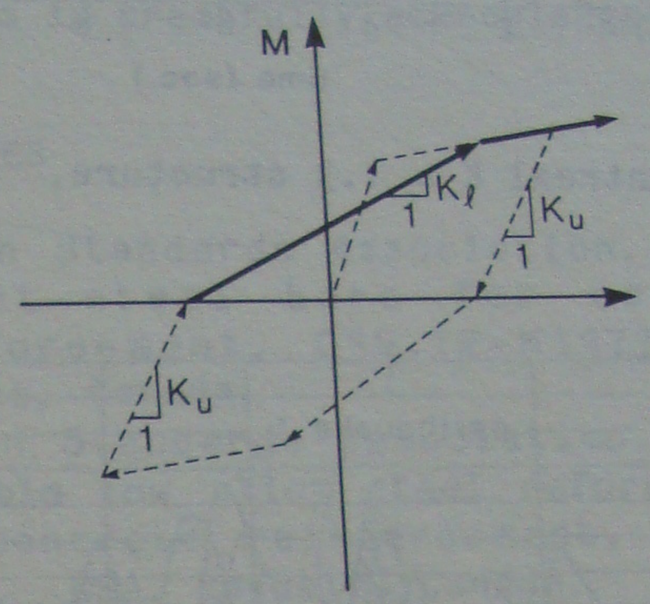

(a) Modified Takeda Model for K = 0.7.

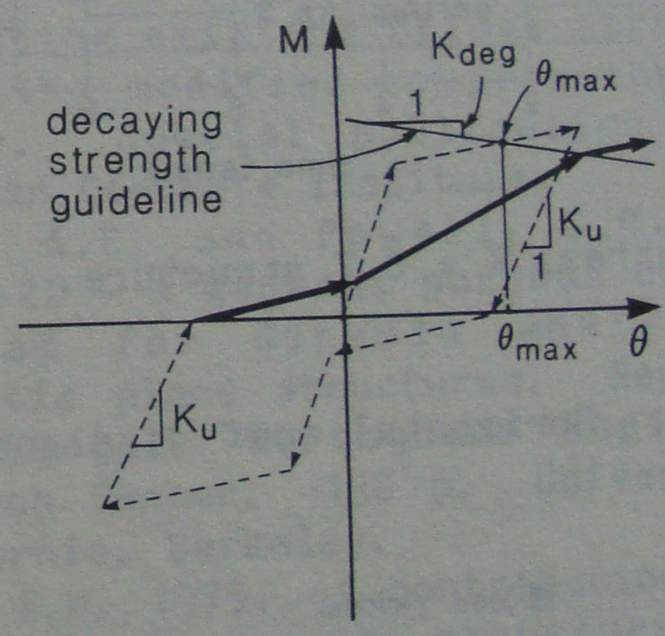

(b) Model for K = 2.0 and K = 1.3.

Fig. 9. Modelling of hysteretic response.

The skeletal curve for the hysteretic responses were determined from the monotonic behavioural predictions previously described. The unloading and reloading stiffnesses were determined from the test results.

Figure 10 gives the roof displacement time history responses for the Montreal K

= 1.3 and K = 0.7 structures. It can be seen that Earthquake 1 and El Centro give about the same maximum displacements for

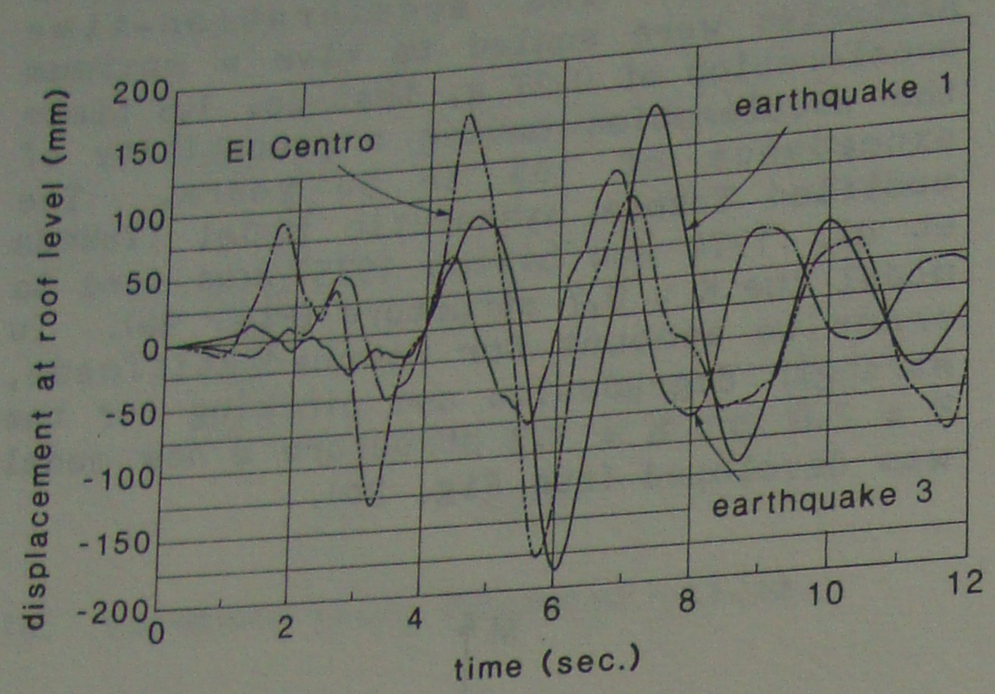

(a) Montreal K = 1.3 structure.

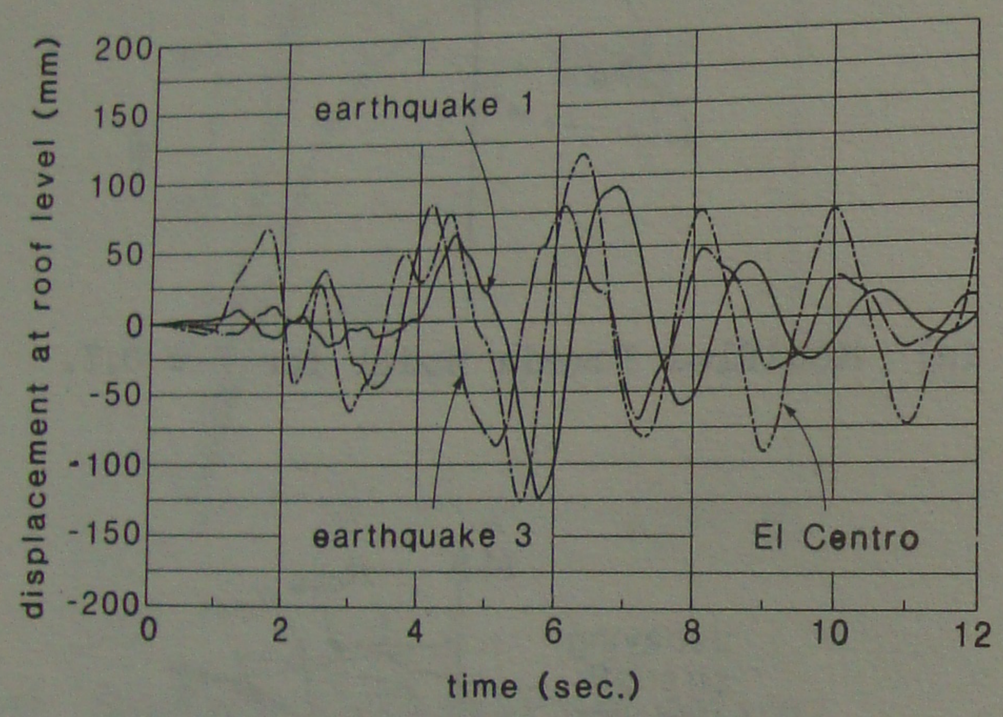

(b) Montreal K = 0.7 structure.

Fig. 10. Horizontal roof displacements.

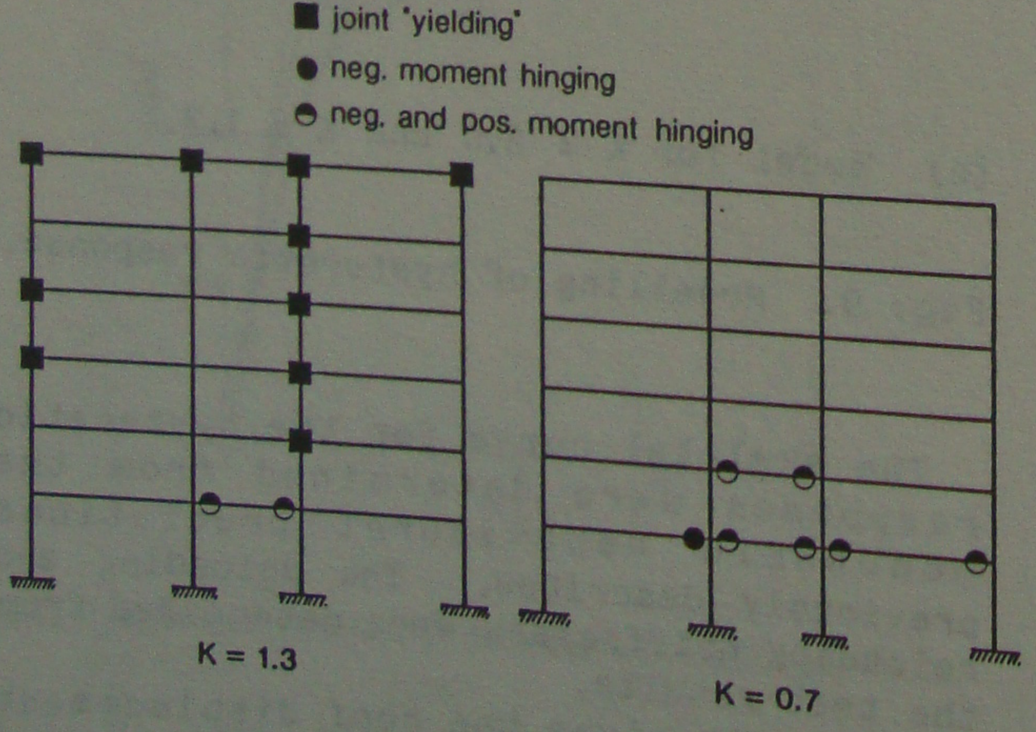

Fig. 11. Hinge locations.

both structures. Structure K = 1.3 experienced a maximum displacement which is 40% greater than that experienced by Structure K = 0.7. This is mainly due to the large number of locations where joint yielding occurred in Structure K = 1.3 as can be seen in Fig. 11. This also resulted in larger interstorey drifts for Structure K = 1.3 as shown in Fig. 12.

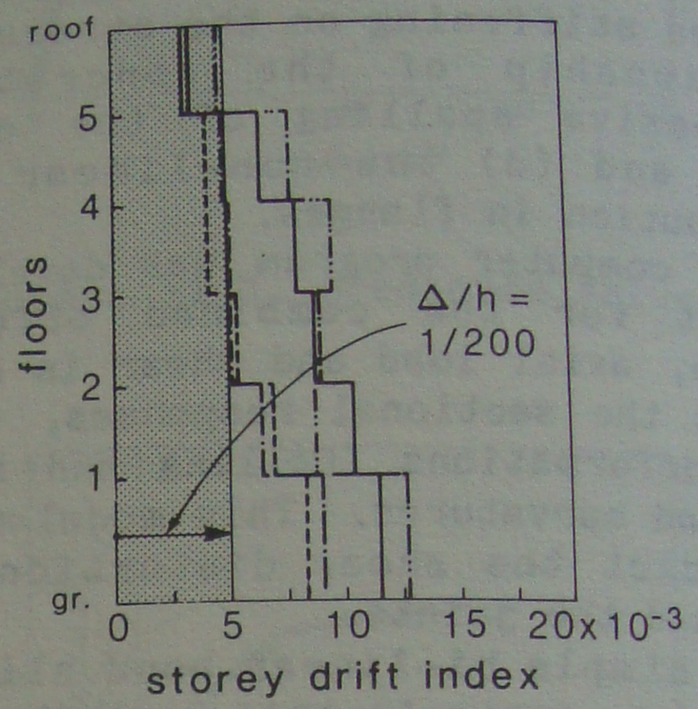

(a) Montreal K = 1.3 structure.

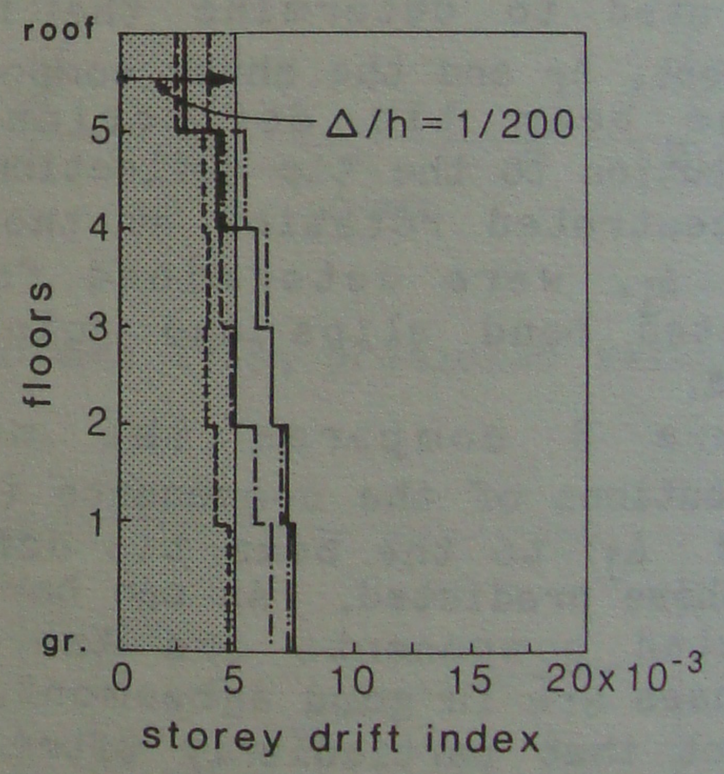

(b) Montreal K = 0.7 structure.

Fig. 12. Interstorey drift envelopes.

Figure 13 compares the predicted shear envelopes with the factored design shear as well as the calculated shear capacity for a typical interior column. As can be seen the shear capacities for these cases were much greater than the demand.

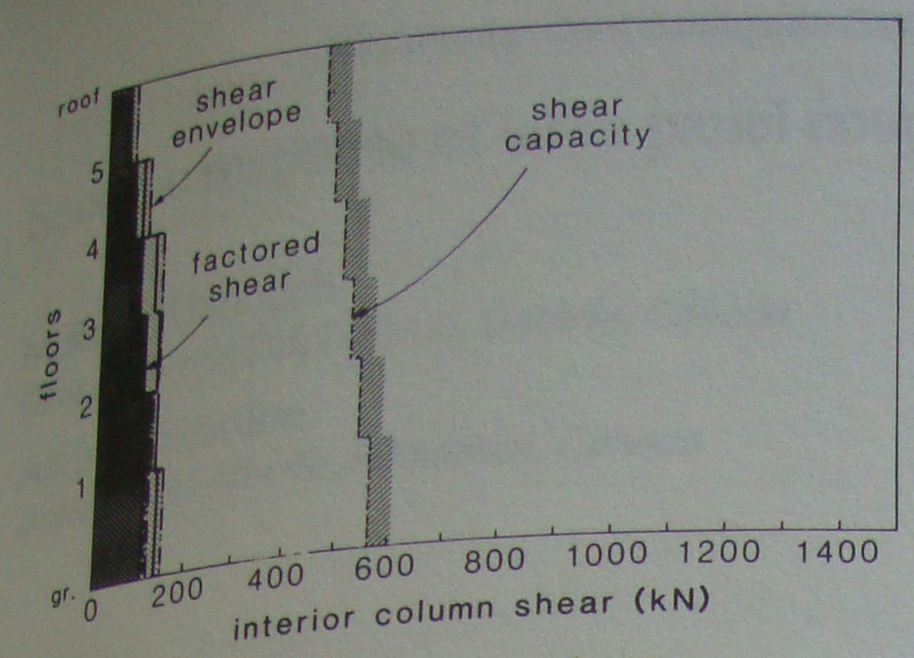

(a) Montreal K = 1.3 structure.

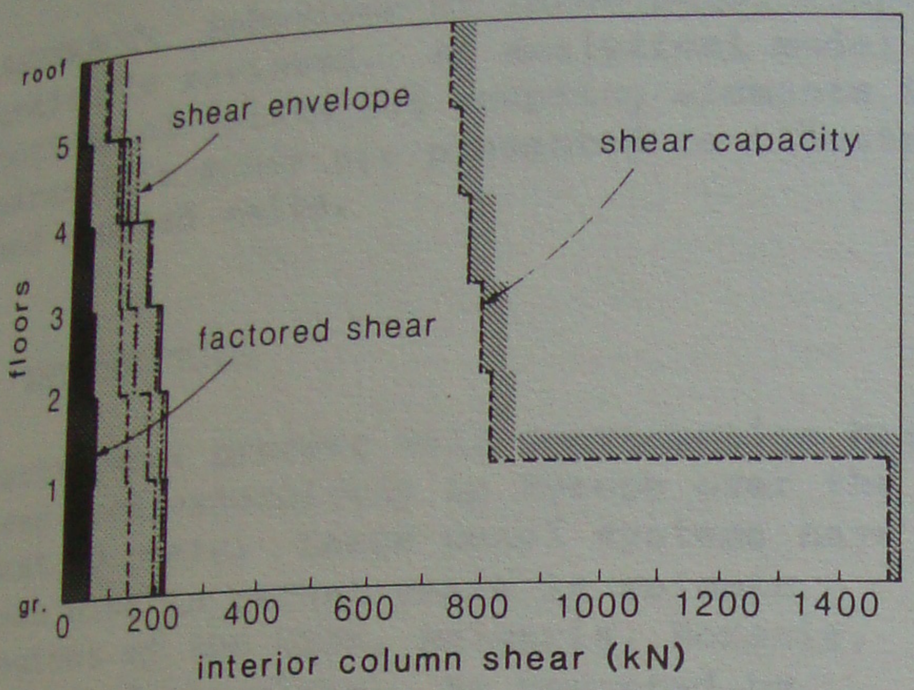

(b) Montreal K = 0.7 structure.

Fig. 13. Shear force envelopes.

7 DESIGN RECOMMENDATIONS AND CONCLUSIONS

The design recommendations and conclusions are summarized below:

1. The tests clearly indicated that the reinforcement in the slab contributes significantly to the response by increasing the "beam" strength and reducing the negative moment ductility.

2. A simple method of determining the "effective slab width" is presented which accounts for the role of the spandrel beam. These effective flange widths can be significantly greater than 3 times the slab width as suggested in the CSA Code (1984).

3. The CSA Code (1984) should be more specific in requiring that all joints be designed to resist at least the factored shear. This study indicates that joint yielding can occur prematurely in K = 2.0 and K = 1.3 structures. The large number of joint failures observed in the 1985 Mexican earthquake (Mitchell 1987) strongly emphasizes the need to address this problem.

4. The K2.0 test specimen had details corresponding to K = 1.3 in previous Canadian concrete codes and displayed little ductility and energy dissipating capacity.

8 ACKNOWLEDGEMENTS

Specimens K1.3 and K0.7 were tested by Suzanne Rattray and Specimen K2.0 was tested by Dan Castele and George Covell. The funding provided by the Natural Sciences and Engineering Research Council of Canada is greatfully acknowledged.

REFERENCES

Canadian Standards Association. 1977a. Billet-steel bars for concrete reinforcement, G30.12-M1977, CSA. Rexdale, Canada.

Canadian Standards Association. 1977b. Weldable low alloy steel deformed bars for concrete reinforcement, G30.16-M1977. CSA. Rexdale, Canada.

Canadian Standards Association. 1984. Design of concrete structures for buildings - CAN A23.3 - M84. CSA. 281 p. Rexdale, Canada.

Collins, M.P. and Mitchell, D. 1985. Evaluating existing bridge structures using the modified compression field theory. Special publication SP-88, American Concrete Institute.

Kanaan, A.E. and Powell, G.H. 1975. DRAIN-2D - A general purpose computer program for dynamic analysis of inelastic plane structures. Report No. EERC 73-22. Earthquake Engineering Research Center. 138 p. University of California, Berkeley.

Litton, R.W. 1975. A contribution to the analysis of concrete structures under cyclic loading. Ph.D. thesis. 146 p. University of California, Berkeley.

Mitchell, D. 1987. Structural damage due to the 1985 Mexican Earthquake. Proceedings of the Fifth Canadian Conference on Earthquake Engineering. Rotterdam: Balkema.

Paultre, P., to be published 1987. An Evaluation of Seismic Performance of Concrete Frame Structures in Canada. Ph.D. thesis, McGill University.

Takeda, T., Sozen, M.A., Nilsen, N.N. 1970. Reinforced concrete response to simulated earthquakes. Journal Structural Division. ASCE. Vol. 96, No. ST 12. p. 2557-2573.